Catal Lett (2008) 123:32–40
DOI 10.1007/s10562-008-9396-6

Ni/Pillared Clays as Catalysts for the Selective Catalytic Reduction of Nitrogen Oxides by Propene

C. Belver · G. Mata · R. Trujillano · M. A. Vicente

Received: 4 September 2007 / Accepted: 4 January 2008 / Published online: 23 January 2008
© Springer Science+Business Media, LLC 2008

Abstract Different and alternative methods for the preparation of Ni/pillared clays based on impregnation and encapsulation procedures are reported. Several nickel precursors and metal loadings are considered in order to evaluate their influence on the structural, textural and catalytic properties of the resulting solids. The behaviour of the optimum solids as catalysts has been proved in the selective catalytic reduction of nitrogen oxides with propene, and the relevance of the oxidant nature was checked by changing the composition of the oxidant mixture. Of all the factors studied, the nature of the nickel precursors appears as the most important one, owing to the formation of different active nickel species during the synthesis procedure.

Keywords Pillared clays · Ni catalysts · DeNO$_x$ reaction

C. Belver
Instituto de Catálisis y Petroleoquímica, CSIC, Campus Cantoblanco, Madrid 28049, Spain

G. Mata · R. Trujillano · M. A. Vicente (✉)
Departamento de Química Inorgánica, Universidad de Salamanca, Salamanca 37008, Spain
e-mail: mavicente@usal.es

G. Mata
e-mail: guiomar@usal.es

R. Trujillano
e-mail: rakel@usal.es

Present Address:
C. Belver
Departamento de Ingeniería Química, Facultad de Químicas, Universidad Complutense de Madrid, Ciudad Universitaria s/n, Madrid 28040, Spain

1 Introduction

Clays are versatile materials employed in diverse applications, comprising from ceramics to catalysts. Their use is mainly based on their properties, surface, acidity and/or composition [1, 2]. In this sense, many tailoring procedures have been performed in order to improve different clays, intercalation-pillaring probably being the one most studied for smectitic group clays [3, 4]. Pillared layered clays appear as new microporous materials whose properties, such as pore size, acidity and redox properties, can be modulated by selecting the adequate synthetic parameters, such as the nature of the pillaring agent, type of clay or thermal treatment, thus opening an important way to design tailored catalysts [5].

The synthesis of pillared clays (PILCs) is based on the ionic exchange of the original interlayer cations by polyoxocations previously prepared by controlled hydrolysis of certain metal cations. The large intercalated polyoxocations are thermally transformed into stable metallic oxidic clusters grafted onto the clay layers, forming interlamellar galleries accessible to small and medium size molecules [6]. The catalytic applications of PILCs depend on the nature of both the parent clay and the intra-layer pillars. The pillar formation allows us to improve the textural properties by the creation of intra-galleries and also to create promising active centers (acidic or metallic). The presence of transition metals (such as Fe, Cr, Co, Cu or Ni), associated with or structurally included in PILCs, has proved to be useful in oxidation–reduction reactions, such as oil cracking, fine chemical synthesis (dehydrogenation, Fischer–Tropsch, etc.) [7, 8] or selective catalytic reduction; in this sense, the literature has reported the application of metal oxide PILCs on the SCR of NO_x with ammonia (NH_3–SCR) or hydrocarbon (HC–SCR) as reductants [9, 10].

NO_x HC–SCR has attracted much attention since it appears as a potential way to remove these pollutants from motor exhausts, avoiding the inconveniences derived from the use of ammonia. So far, the most common De–NO_x catalysts employed are based on transition and noble metals supported over zeolites or alumina [11–13]. The use of metal pillared clays in this reaction has not been extended, a few reports based on Fe-, Co-, Cr-, Ti- and Cu-PILCs [14–18], and more recently noble metal PILCs having been published [19]. We have focused our attention both on pillared clays, as optimum microporous materials for this reaction, and on Ni-catalysts, described in the literature as effective for NO_x reduction in presence of C_2 and C_3 hydrocarbons [20, 21].

Thus, we have prepared Ni/saponite catalysts by two different methods; impregnation of Al-pillared saponite with several nickel precursors, and encapsulation of nickel complexes in parent and in intercalated clay. The resulting materials were characterized and evaluated as catalysts for selective catalytic reduction of nitrogen oxides with propene. It has been reported that when the reaction is performed in the presence of oxygen there is a competitive hydrocarbon oxidation between two possible reactions: on the one hand, the oxidation by NO_x and O_2 to produce N_2 (actually, the objective of the SCR reaction), and on the other hand, the oxidation by O_2 alone (which can be considered an undesirable competitive oxidation) [22]. In order to gain information on the mechanism of the reaction, it was carried out using an $NO_x + O_2$ mixture or pure O_2 as oxidants.

2 Experimental

2.1 The Starting Clay

The clay used in this work was the saponite from Cabañas (Toledo, Spain), supplied by TOLSA (Madrid), previously purified by dispersion–decantation of the <2 μm fraction [23]. Its cation exchange capacity was 0.99 mequiv/g, its basal spacing 12.2 Å and the BET specific surface area 191 m^2/g.

2.2 Synthesis of Ni–Clay Catalysts

The synthesis of the Al-pillared saponite was carried out by intercalation of Al_{13} polycations using a standard procedure [24]. Al_{13}^{7+} polycations were prepared by controlled hydrolysis of an Al^{3+} solution (obtained from $AlCl_3{\cdot}6H_2O$) with 1 M NaOH, using a ratio of $OH^-/Al^{3+} = 2.2$. The hydrolysis reaction was maintained under vigorous stirring during 24 h. Then, the solution was added to a previously prepared clay suspension employing an Al/clay ratio of 5 mmol/g, aging the new suspension under stirring for 24 h. The resulting solid was separated by centrifugation, washed by dialysis, dried overnight at 70 °C and finally calcined at 500 °C for 2 h. The sample thus synthesized, pillared saponite, was designated as Al-PILC (in some cases, we use the term Al-intercalated saponite to refer to the sample before calcination, only dried).

The Al-pillared saponite synthesized above was used as support for the preparation of the first series of nickel catalysts. Nickel was incorporated by a standard incipient wetness impregnation method [25]. Thus, Ni(II) nitrate, Ni(II) chloride and Ni(II) acetylacetonate salts (Sigma-Aldrich) were chosen as Ni(II) precursors. Impregnation with Ni chloride was performed in order to obtain catalysts with NiO loading from 1 to 3 wt.%; nevertheless, preliminary catalytic results made it necessary to increase the nickel amounts to obtain catalysts with NiO loading from 1.5 to 6 wt.%. The precursors were dissolved in the minimum solvent amount (acetone for acetylacetonate salt and water for the rest) and the solution was added to the Al-PILC support. The resulting solids were dried and calcined following the same protocol reported above. The solids were designated as follows: *Ni(nit)*, *Ni(acac)* and *NiCl*, indicating the metal precursor, Ni(II) nitrate, acetylacetonate and chloride, respectively; followed by a number that indicates the formal NiO load of the catalyst.

The second series of nickel catalysts was prepared by encapsulation of a nickel complex in the natural or in the Al-intercalated saponite. This procedure was developed in order to combine the chemical selectivity of the metal complex with the stability of heterogeneous supported catalysts [26]. Thus, Ni(II) phtalocyanine (Sigma-Aldrich) was chosen as Ni-complex using pyridine (Sigma-Aldrich) as solvent. The encapsulation procedure was performed by putting the clay in touch with a large amount of the complex for 72 h, replacing the evaporated solvent during the process. The solids obtained were separated by filtration, dried and calcined in the same way as the other nickel samples. The solids were named *Ns* or *Is*, indicating the clay support (natural or intercalated saponite, respectively), followed by the abbreviation of the metal complex, *Ph*. Almost all data given correspond to the samples calcined at 500 °C, which are the final catalysts; when we refer to dried samples, before calcination, the suffix *dried* is added to the name.

2.3 Characterization of the Solids

Elemental analyses were carried out by Activation Laboratories Ltd., Ancaster, Ontario, Canada, using Inductively Coupled Plasma Optical Emission Spectroscopy (ICP OES).

Powder X-ray diffraction (PXRD) patterns were registered between 2 and 70° (2θ) with a scanning velocity of 2°/min by using a Siemens D-500 diffractometer, operating at 40 kV and 30 mA, and employing Cu Kα filtered radiation ($\lambda = 1.5418$ Å). The equipment was connected to a DACO-MP microprocessor and used Diffract-AT software.

Textural analyses were carried out with nitrogen adsorption–desorption isotherms at −196°C using a Micromeritics apparatus (ASAP 2010). The samples were degassed for 6 h at room temperature and then for 2 h at 110 °C. Specific surface areas were obtained from the BET method, microporous surface area by means of the *t* method, and total pore volume from the adsorption at p/p^0 0.99.

DR-UV–Vis spectra were recorded in reflectance mode by using a Shimadzu spectrometer UV-2100, with an optical length of 0.4 cm.

2.4 Catalytic Activity

The catalytic properties of the Ni/clays have been tested for the selective catalytic reduction of nitrogen oxides. The reducing agent chosen for this work was propene, a common hydrocarbon model used in the literature for testing HC-SCR. The activity of each Ni/catalyst was measured in a fixed bed flow reactor using a catalytic bed composed of the sieved catalyst (125–250 μm particle size range) mixed with SiC (ratio 1/2 catalyst vs. SiC). The catalyst amount and the total flow were adjusted in order to work with a gas hourly space velocity of 50,000 h^{-1} (catalyst, 0.6 g; total flow rate, 500 cm^3/min). The HC-SCR reaction was evaluated under stoichiometric conditions, adjusting the reactant gas (v/v) at 0.1% C_3H_6 (L'Air Liquide), 0.45% NO_x (NO 98%; NO_2 1%; N_2O 0.5%, Carburos Metálicos) and 0.225% O_2 (L'Air Liquide), employing nitrogen as effluent (L'Air Liquide). The relevance of the presence of oxygen in this reaction was evaluated by introducing only oxygen to the inflow gas; this case was also performed under stoichiometric ratios adjusting the reactant mixture to 0.1% C_3H_6 and 0.45% O_2.

The reaction was carried out under stationary conditions from 200 to 500 °C, using a heating rate of 5 °C min^{-1} and a stabilization time of 25 min, recording data at intervals of 50 °C. The outflow gas was analysed by on-line infrared spectroscopy using a Perkin-Elmer 1725X FTIR spectrometer with a multiple reflection transmission cell (Infrared Analysis Inc.), analyzing the infrared bands from C_3H_6, NO_x (NO, N_2O, NO_2), CO_2 and CO. Catalytic activities for NO_x were evaluated in terms of percentage conversions of NO and NO_2 to N_2, because N_2O formation was negligible in all the conditions studied.

3 Results and Discussion

3.1 Characterization of Ni-clays

The intercalation-pillaring process with aluminum-polycations was successful, increasing the basal spacing from 13.8 Å ($2\theta = 6.39°$) in the natural clay to 18.2 Å ($2\theta = 4.85°$) in the intercalated solid and 17.8 Å ($2\theta = 4.96°$) in the pillared one (Fig. 1).

The impregnated samples maintain the layered structure of the Al-PILC support although the *c*-axis ordering decreases, indicating some delamination after impregnation (Fig. 1). The behaviour of the three nickel precursors is quite similar, suggesting a high dispersion of the Ni species on the support surface; only impregnation with high amounts of acetylacetonate causes the formation of detectable crystallites of NiO bunsenite phase (JCPDS: 4-0835), see the Ni(acac)6 diffractogram. This could be due to a more rapid crystallization of nickel during the impregnation with this precursor, because of the high volatility of the acetone used as solvent.

The encapsulation process leads to solids with a basal spacing of 13.1 Å, with a shoulder at 14.6 and 12.9 Å, respectively, when using both supports, natural and Al-intercalated saponite, together with all the characteristic peaks from the supports and from the Ni-complex (Fig. 2). For intercalated saponite, it is evident that the interaction with the organic molecule provokes the collapse of Al_{13}^{7+} units; the 001 reflection peak is observed at lower basal spacing, that is, at the spacing characteristic of non-pillared clay. It may be considered that on this support the Al_{13} species have still not been transformed into pillars and are

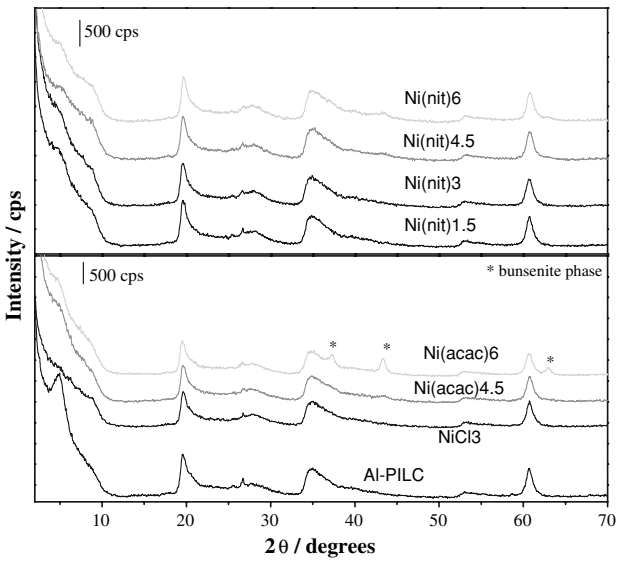

Fig. 1 XRD patterns of some impregnated solids; the diffractogram of the support, Al-PILC solid, is shown as reference

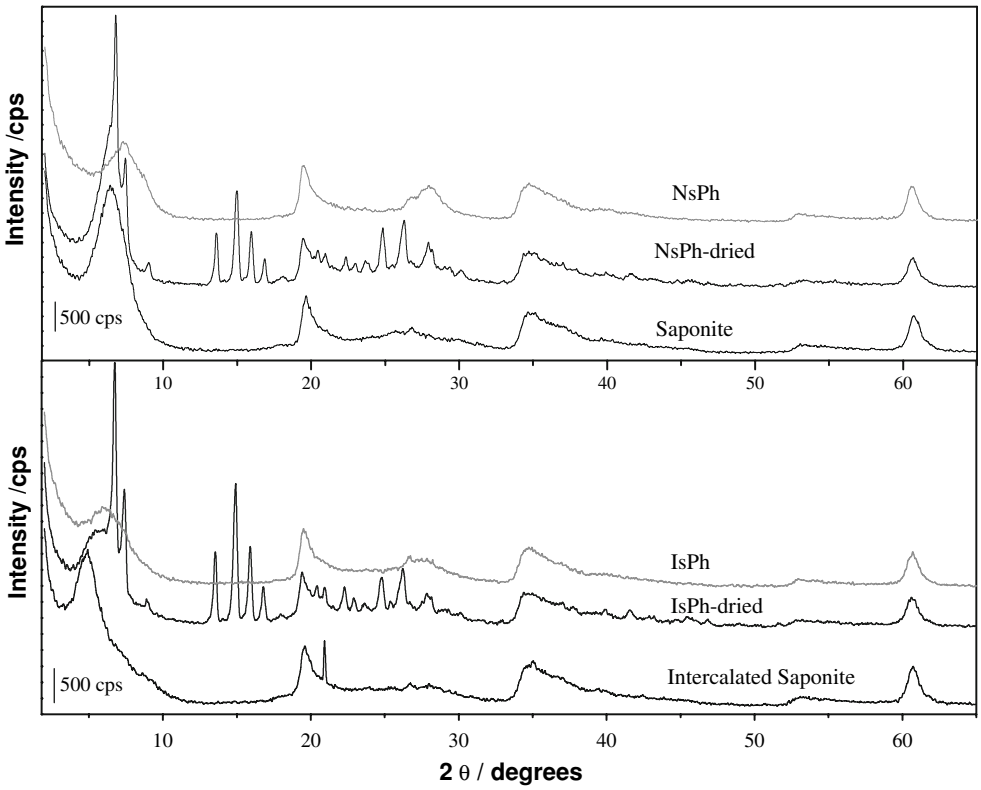

Fig. 2 XRD patterns of the encapsulated solids; the diffractograms of parent and intercalated saponite are shown as reference

not linked to the clay layers but as polycationic species. Looking at the chemical composition of the solids and the thermal analyses (not shown), it is deduced that the nickel complex is situated in the interlayer space of natural saponite by substitution of water molecules, being intercalated as neutral molecules; cationic exchange is not observed. As water is removed, the basal spacing of the intercalated solids can be compared to the TOT height of saponite (9.6 Å) and the separation of the layers produced by the complex was 3.3–3.5 Å (the TOT separation is the height of the individual layers of the clay, composed of an octahedral sheet sandwiched between two tetrahedral sheets [TOT notation]. Thus, it is the basal spacing when there is no molecule in the interlayer, in the case of saponite having, as indicated, a value of 9.6 Å). In our case, the form of the molecule of the precursor allows a large number of them to be packed in the interlayer spacing, giving rise to a high final nickel content. When these solids are calcined at 500 °C, the characteristic diffractogram of the clay is observed, with intense peaks at 14.6 and 12.0 Å, not showing any effect due to the formation of NiO crystallites.

The chemical analyses of the parent clay and of the Al-PILC solid (Table 1) show the increase in Al_2O_3 content, and the decrease of CaO and, to a lesser extent, of K_2O, confirming the cation exchange between Al_{13}^{7+} and the exchangeable cations of the clay. On the other hand, the chemical composition of the impregnated solids shows that the NiO contents are close to the formal percents targeted. The two samples prepared by encapsulation show very different behaviours. Whereas the one prepared using natural clay fixes 7.0% NiO, the sample prepared from the intercalated clay fixes a very low amount, only 0.003% NiO. It seems that Ni(II) phtalocyanine easily enters into the interlayer region when using the natural clay, but this is not possible when using the intercalated one, the traces of NiO detected probably being due to a small retention on the external surface of the clay. However, this does not explain why the expanded layered structure of the intercalated clay strongly collapses in contact with the Ni(II) phtalocyanine solution.

The nitrogen adsorption–desorption isotherms of all solids are of type II (IUPAC classification, not shown) with a type H3 hysteresis loop and a high adsorption at low relative pressures. This behaviour is characteristic of layered materials with slit-like pores and microporosity [27, 28]. The textural parameters of the solids obtained from these isotherms are listed in Table 2.

Natural saponite shows a high specific surface area value, characteristic of saponites in the Madrid Basin, owing to their small particle size, derived from the sedimentary origin of these deposits [29, 30]. The specific surface area and the microporosity increase from the natural clay (191 $m^2\ g^{-1}$) to the pillared solid (230 $m^2\ g^{-1}$). After the impregnation procedure, these values decrease in all cases, which may be caused by to two effects. First, Ni species occupy a certain amount of the surface of the solid,

Table 1 Chemical composition of the natural clay, the pillared clay and the nickel samples (wt. %, water free solids)

Sample	SiO_2	Al_2O_3	Fe_2O_3	MnO	MgO	CaO	Na_2O	K_2O	TiO_2	NiO
Saponite	58.8	6.3	1.9	0.11	31.4	0.49	0.08	0.55	0.25	–
Al-PILC	54.6	14.4	1.8	0.10	28.1	0.02	0.09	0.44	0.22	–
NiCl1	54.5	15.1	1.9	0.11	26.4	0.03	0.08	0.58	0.24	0.9
NiCl1.5	53.8	15.0	2.3	0.11	26.2	0.03	0.08	0.61	0.24	1.5
NiCl2	53.5	14.8	1.7	0.11	26.0	0.03	0.07	0.55	0.23	2.8
NiCl3	52.8	14.9	2.2	0.10	25.9	0.03	0.08	0.59	0.23	3.3
Ni(acac)1.5	54.4	15.0	2.2	0.11	26.4	0.03	0.08	0.59	0.24	1.08
Ni(acac)3	53.1	14.7	2.0	0.10	25.9	0.03	0.08	0.60	0.23	3.2
Ni(acac)4.5	53.1	14.7	1.7	0.10	25.8	0.03	0.08	0.55	0.23	3.5
Ni(acac)6	51. 9	14.4	1.7	0.10	25.3	0.03	0.08	0.56	0.23	5.6
Ni(nit)1.5	53.3	14.7	3.3	0.10	25.9	0.03	0.08	0.54	0.23	1.7
Ni(nit)3	53.6	14.8	1.6	0.10	26.1	0.02	0.08	0.60	0.23	2.7
Ni(nit)4.5	52.2	14.5	2.2	0.10	25.5	0.02	0.07	0.58	0.23	4.4
Ni(nit)6	51.9	14.4	1.8	0.10	25.4	0.03	0.08	0.62	0.23	5.3
NsPh	53.2	6.4	2.0	0.12	29.6	0.51	0.11	0.63	0.25	7.0
IsPh	55.0	15.4	2.1	0.09	26.2	0.14	0.23	0.05	0.28	0.003

Table 2 BET specific surface area (S_{BET}), microporous surface area (S_{MP}) and total pore volume (V_T) of the solids indicated

Sample	$S_{BET}/m^2\ g^{-1}$	$S_{MP}/m^2\ g^{-1}$	$V_T/cm^3\ g^{-1}$
Saponite	191	143	0.157
Al-PILC	230	180	0.176
NiCl1	159	115	0.137
NiCl1.5	145	104	0.128
NiCl2	137	100	0.121
NiCl3	102	71	0.102
Ni(acac)1.5	182	129	0.167
Ni(acac)3	186	131	0.167
Ni(acac)4.5	183	131	0.165
Ni(acac)6	183	131	0.166
Ni(nit)1.5	169	123	0.147
Ni(nit)3	154	113	0.134
Ni(nit)4.5	151	118	0.126

and block the entrance to a certain amount of its porosity. And second, a new calcination is carried out after impregnation to produce the final catalysts, this new calcination obviously having a deleterious effect on the textural properties of the solid. All nickel catalysts possess optimum surface areas and microporosity for catalytic applications. The acetylacetonate impregnation appears as the best way to obtain materials with high surface areas, around 180 $m^2\ g^{-1}$ with 70% of microporous surface area. Both encapsulated solids, also studied after calcination at 500 °C, have very similar textural parameters, with the surface area close to 137 $m^2\ g^{-1}$.

The nickel species present in the samples were studied by DR-UV–Vis spectroscopy; the electronic spectra of the impregnated samples are shown in Fig. 3.

The nickel-supported solids exhibit electronic spectra similar to the support (Fig. 3a, b); only in the derivative curves is it possible to observe some differences (Fig. 3c, d). According to the literature, it is possible to distinguish the d–d transitions of Ni^{2+} ions in different environments [31, 32]. An absorption band appears around 350 nm, attributed with the $^3A_{2g} - {}^1T_{1g}$ (D) transition of octahedral Ni(II) in NiO. At higher wavelengths, and overlapping with an absorption band of the Al-PILC, a shoulder becomes visible at around 590–650 nm, probably associated to the $^3T_1$–$^1T_2$ and $^3T_1$–$^3T_1$ (P) transitions of tetrahedral Ni(II) ions in the alumina lattice, attributed to the presence of $NiAl_2O_4$ spinel [33]. Comparing the impregnated solids, the Ni(nit) series only shows evidence of these absorption bands in the samples with high nickel content (3%), as also occurs for the NiCl series, while in the Ni(acac) series, this absorption becomes more evident. If Fig. 3d is analysed in detail, it is possible to observe that the band of the support at 400 nm almost disappears in the Ni(acac)4.5 sample, another one appearing at 390 nm in the Ni(acac)6 sample. According to the literature, this band is attributed to the presence of $NiAl_2O_4$ spinel, assigned to the $^3A_{2g}$–$^1T_{1g}$ (P) transition of octahedral Ni(II) in the alumina lattice [33]. The Ni(acac)6 solid also presents another band at 715 nm, probably associated with the $^3A_{2g}$–$^3T_{1g}$ (F) transition of octahedral Ni(II) in NiO. These results suggest that the impregnation preparation process yields similar nickel species for all samples, the Ni(II) acetylacetonate being the optimum precursor for obtaining higher amounts of NiO and $NiAl_2O_4$ species, whose presence could be relevant for catalytic applications. The encapsulated samples could not be studied by this technique owing to their intense black colour, which produces a continuous light absorption.

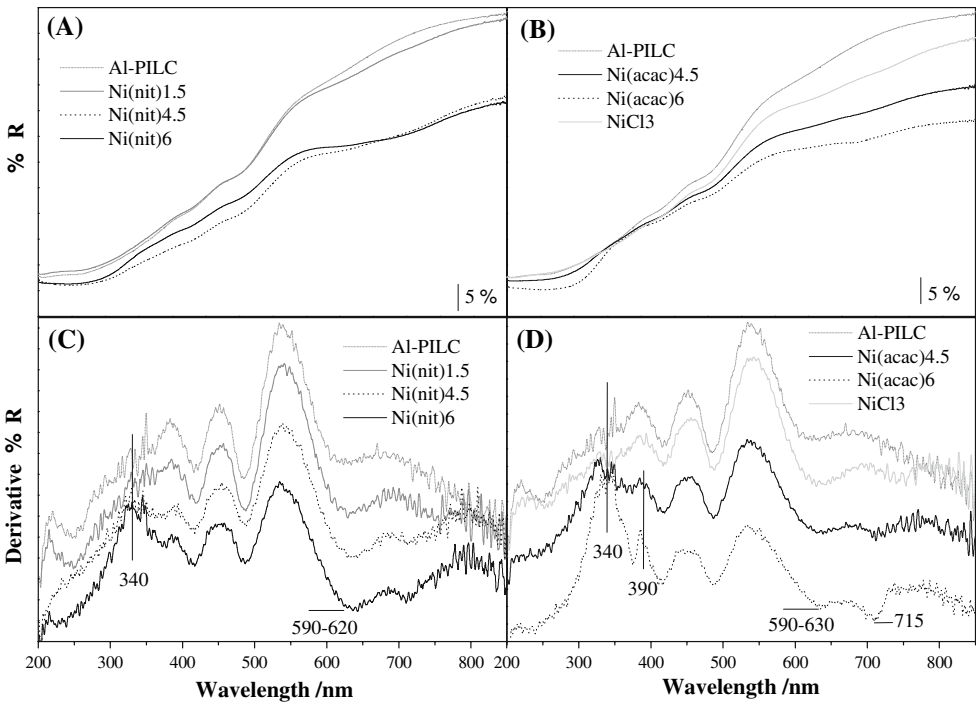

Fig. 3 DR-UV–Vis spectra of impregnated solids (**a**, **b**) and their respective derivative curves (**c**, **d**)

3.2 Catalytic Properties: Selective Catalytic Reduction of Nitrogen Oxides

The NO_x reduction with propene in the presence of oxygen yields the same products for all solids studied, N_2, CO_2 and carbon deposits; without detection of N_2O, NH_3 or CO as by-products. The nitrogen oxides and propene conversion values are plotted in Fig. 4 versus the reaction temperature for the catalysts with analogous metal loads prepared by impregnation from different nickel precursors, together with the values given by a solid prepared using the encapsulation procedure.

The catalytic activity of the support, Al-PILC solid, is given for comparison. This solid shows a low conversion, about 5%, which confirms that Ni-species are the main ones responsible for the catalytic activity of the solids; NO_x and propene conversions are quite similar for the different solids, only the solids impregnated with acetylacetonate appear as more active. Propene conversion reaches values of 30%, whereas the nitrogen oxides reduction only reaches 19%. Although these data are not as high as others described for nickel catalysts [22, 34], they are analogous to those displayed for NiO and some Ni-ZSM-5 catalysts [32, 35]. The formation of carbonaceous species during the reaction seems to be the main reason for this low activity; it is known that the formation of these species is not easily reversible [36]. The main difference between the samples considered is related to the nature of the nickel precursor, Ni(acac) being the most active series (Fig. 4). In this sense, the literature has reported that the SCR activity is related to the presence of NiO and $NiAl_2O_4$ species [20], although the acidity properties also possess relevance [34]. The presence of a highly dispersed NiO phase has mainly been related to C_3H_6 oxidation. On the other hand, the catalytic relevance of metal aluminates has been suggested by different authors, considering that transition metal cations located in surface aluminate exhibited lower reducibility than those in bulk oxide particles. Hence, the non-selective reaction of hydrocarbon with oxygen is decreased, and the desired NO_x reduction is achieved [32, 37]. Thus, the major presence of NiO and $NiAl_2O_4$ in the solids derived from Ni(acac) could explain the activity of this series. However, the synthesis method does not appear to be an important factor in the optimization of the catalytic properties of the solids. The encapsulation procedure does not lead to better activities than the impregnation process, even though the encapsulated sample has higher nickel content. The encapsulated sample only shows higher activities than the series prepared from the nitrate precursor, probably owing to the nickel species formed after thermal treatment.

In order to study the selectivity of the hydrocarbon as a reducing agent of the nitrogen oxides, pure oxygen was tested as oxidant. The conversion values of some of the catalysts are plotted in Fig. 5.

Clearly, the oxidation activity curve for the reaction C_3H_6–NO_x–O_2 becomes separated from the C_3H_6–O_2 reaction curve at low temperatures. The hydrocarbon conversion reaches higher values with $NO_x + O_2$ than with pure O_2 when the reaction temperature is below 400 °C, except for the Ni(acac)4.5 sample, where both conversion

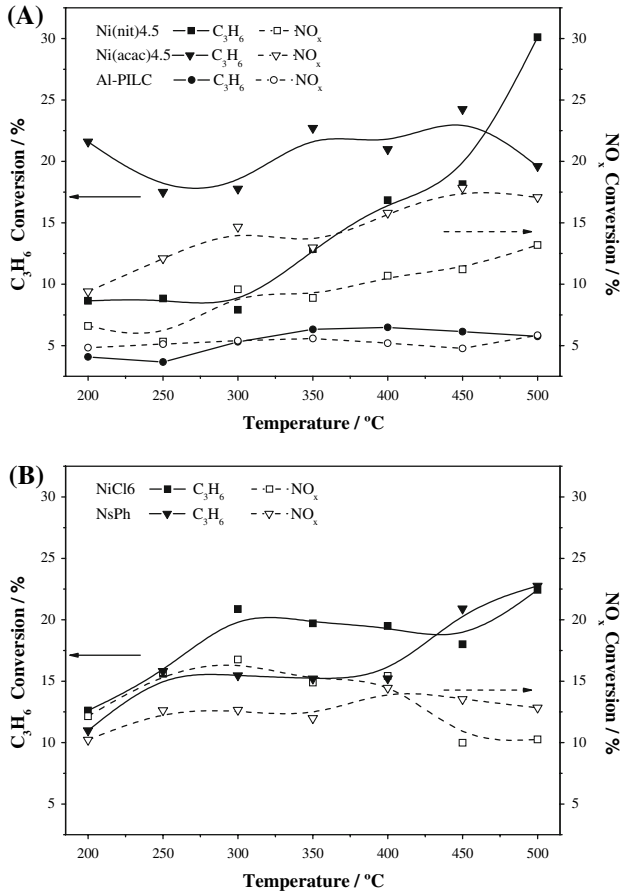

Fig. 4 Hydrocarbon and NO_x conversion values comparing the Ni-precursor and the synthesis procedure for similar nickel contents; (**a**) Ni(nit)4.5 and Ni(acac)4.5 samples, Al-PILC results are shown as reference; (**b**) $NiCl_6$ and NsPh samples

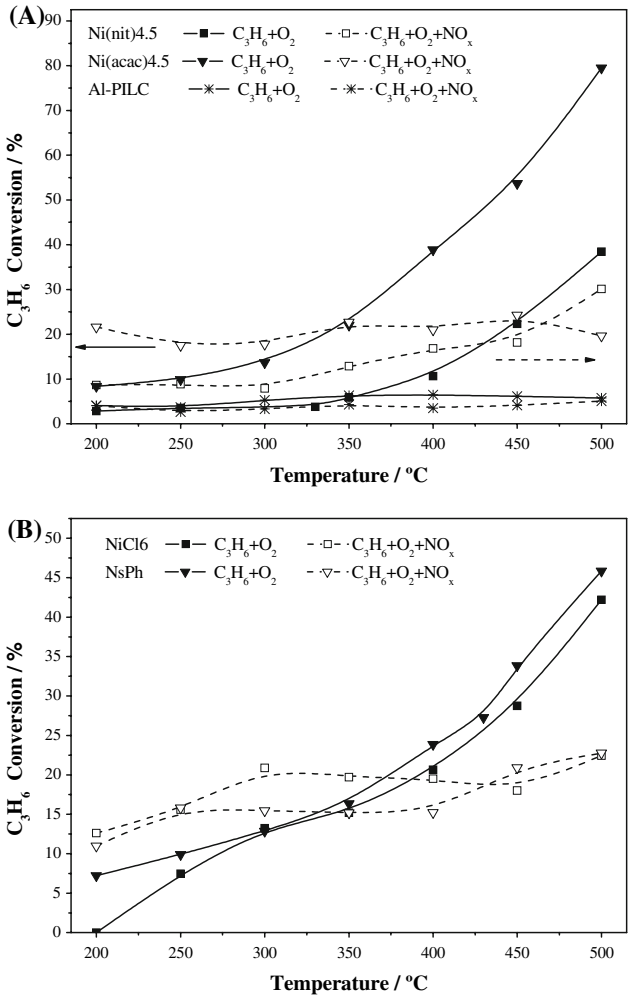

Fig. 5 Propene conversion values versus reaction temperature for C_3H_6–NO_x–O_2 and C_3H_6–O_2 reactions; (**a**) Ni(nit)4.5 and Ni(acac)4.5 samples; Al-PILC results are shown as reference; (**b**) NiCl6 and NsPh samples

curves cross around 300 °C. Nevertheless, when the temperature reaches higher values the hydrocarbon conversion is favoured when using only oxygen in the effluent gas. This behaviour suggests that the selective suppression of the C_3H_6–O_2 reaction is only possible at reaction temperatures below 400 °C, when the C_3H_6–NO_x–O_2 reaction yielding N_2 is enhanced. In this sense, the nature of the nickel precursor appears as an important factor, the Ni(nit) series being the most efficient for this purpose. Although not shown, the C_3H_6–O_2 reaction causes the partial oxidation of propene, CO appearing as product at temperatures higher than 450° C, and being more evident for the more active samples (0.1% for Ni(acac)4.5). Nevertheless, no detection of CO is observed for the C_3H_6–NO_x–O_2 reaction; in this case it is possible to enhance the propene mineralization.

The influence of the Ni content was analysed by comparing the catalytic activity of the solids of a given series, that is, prepared from the same precursor but varying the Ni content. The series prepared from Ni-nitrate was considered, its results being given in Fig. 6. These results show a slight increase in the activity for hydrocarbon oxidation when increasing the amount of Ni, reaching a maximum located at 4 wt.%, while the reduction of NO_x only changes at the higher nickel contents. Although the literature describes an increasing activity related to the nickel loading in zeolites (associated with the amount of disperse Ni^{2+} cations [35, 36]), it is important to indicate that the NO_x reduction is typically limited by the availability of a reducing agent [34]. Therefore, our results suggest that at low-medium nickel contents the concentration of the reducing agent at the active sites is insufficient.

4 Conclusions

Treatment of natural or pillared saponite with nickel precursors successfully yields layered solids with high surface

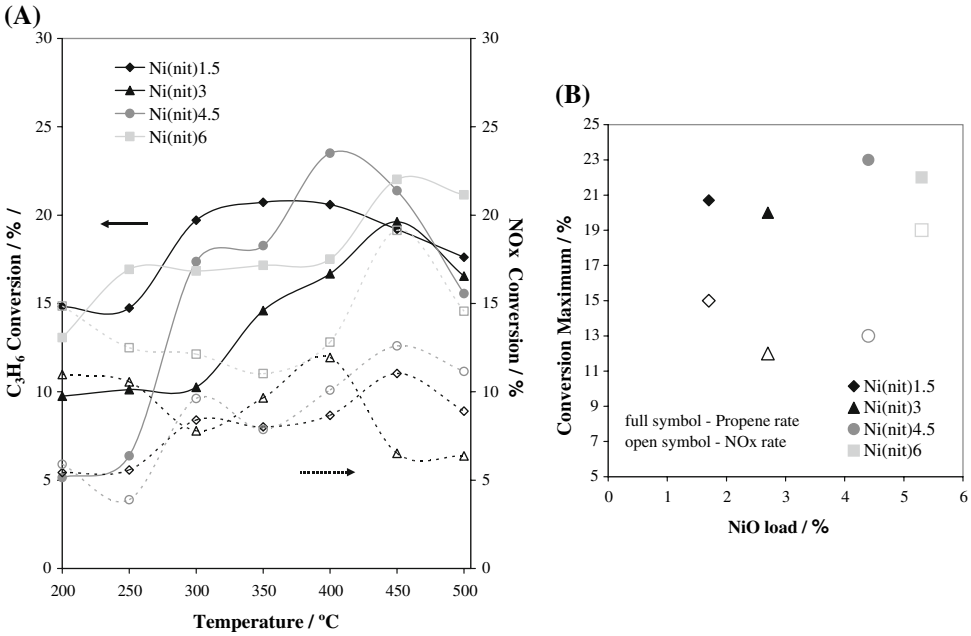

Fig. 6 Hydrocarbon and NO_x conversion for the Ni-nitrate series comparing the nickel loading: (**a**) following the reaction from 200 to 500 °C; (**b**) maximum conversion values

area, microporosity and controlled nickel amounts. Their characterization showed the presence of two types of nickel species with catalytic activities.

The resulting solids present, for the selective catalytic reduction of nitrogen oxides, a behaviour similar to that of other nickel catalysts based on zeolitic supports. Optimization of the reaction rates and enhancement of the reduction of nitrogen oxides to nitrogen can be achieved by suppressing the competitive hydrocarbon oxidation, which is found by choosing the adequate nickel precursor and the reaction conditions.

Acknowledgments The authors thank the financial support of this work from the Junta de Castilla y León and FEDER funds (SA101A07) and the Ministerio de Educación y Ciencia and FEDER funds (MAT2007-66439). R.T. thanks MEC for a contract from the *Ramón y Cajal* Program, and C.B. thanks the MEC for a contract from the *Juan de la Cierva* Program. Special thanks are given to the J. Soria group for the use of the catalytic test equipment.

References

1. Vaccari A (1999) Appl Clay Sci 14:161
2. Murray HH (2000) Appl Clay Sci 17:207
3. Ding Z, Kloprogge JT, Frost RL, Lu GQ, Zhu HY (2001) J Porous Mater 8:273
4. Serwicka EM, Bahranowski K (2004) Catal Today 90:85
5. Gil A, Gandia LM, Vicente MA (2000) Catal Rev 42:145
6. Kloprogge JT (1998) J Porous Mater 5:5
7. Kloprogge JT, Duong LV, Frost RL (2005) Environ Geol 47:967
8. Varma RS (2002) Tetrahedron 58:1235
9. Long RQ, Yang RT, Zammit KD (2000) J Air Waste Manage 50:436; Yang RT, Cichanowicz J (1995) US Patent No. 5,415,850
10. Valverde JL, de Lucas A, Sánchez P, Dorado E, Romero A (2003) Appl Catal B 43:43
11. de Lucas A, Valverde JL, Dorado F, Romero A, Asensio I (2005) J Mol Catal A 225:47
12. Burch R (2004) Catal Rev 46:271
13. She X, Flytzani-Stephanopoulos M (2006) J Catal 237:79
14. Belver C, Vicente MA, Martínez-Arias A, Fernández-García M (2004) Appl Catal B 50:227
15. Mata G, Trujillano R, Vicente MA, Belver C, Fernández M, Korili SA, Gil A (2005) Appl Catal A 327:1
16. Valverde JL, de Lucas A, Dorado F, Romero A, García PB (2005) J Mol Catal A 230:23
17. Long RQ, Yang RT (1999) Catal Lett 59:39
18. De Stefanis A, Tomlinson AAG (2006) Catal Today 114:126
19. Mendioroz S, Martín-Rojo AB, Rivera F, Martín JC, Bahamonde A, Yates M (2006) Appl Catal B 64:161; Mohino F, Avila P, Salerno P, Bahamonde A, Mendioroz S (2005) Catal Today 107:192
20. Meng M, Lin P, Fu Y (2001) Spectrosc Lett 34:83
21. Zhang SJ, Li LD, Zhang FX, Xue B, Guan NJ (2005) Chinese J Catal 26:929
22. Okazaki N, Katoh Y, Shiina Y, Tada A, Iwamoto M (1997) Chem Lett 26:889
23. Toranzo R, Vicente MA, Bañares-Muñoz MA (1997) Chem Mater 9:1829
24. Lahav N, Shani U, Shabtai J (1978) Clays Clay Miner 26:107
25. Che M, Clause O, Marcilly Ch (1999) In: Ertl G, Knözinger H, Weitkamp J (eds) Preparation of solid catalysts, Wiley-VCH, Weiheim
26. Cardoso B, Pires J, Carvalho AP, Kuzniarska-Biernacka I, Silva AR, de Castro B, Freire C (2005) Micropor Mesopor Mater 86:295
27. Sing KSW, Everett DH, Haul RAW, Moscou L, Pierotti RA, Rouquerol J, Siemieniewska T (1985) Pure Appl Chem 57:603
28. Rouquerol F, Rouquerol, Sing K (1999) Adsorption by powders and porous solids. Principles, methodology and applications. Academic Press, London
29. Casal B, Merino J, Ruiz-Hitzky E, Gutiérrez E, Alvarez A (1997) Clay Miner 32:41
30. Prieto O, Vicente MA, Bañares-Muñoz MA (1999) J Porous Mater 6:335
31. Utchariyajit K, Gulari E, Wongkasemjit S (2005) Appl Organomet Chem 20:81

32. Zhang SJ, Li LD, Xue B, Chen JX, Guan NJ, Zhang FX (2006) Reac Kinet Catal Lett 89:81
33. Jitianu M, Jitianu A, Zaharescu M, Crisan D, Marchitan R (2000) Vib Spectrosc 22:75
34. Mosqueda-Jiménez BI, Jentys A, Seshan K, Lercher JA (2003) Appl Catal B 43:105
35. Mihaylov M, Hadjiivanov K, Panayotov D (2004) Appl Catal B 51:33
36. Mosqueda-Jiménez BI, Jentys A, Seshan K, Lercher JA (2003) J Catal 218:375
37. Shimizu K, Maeshima H, Satsuma A, Hattori T (1998) Appl Catal B 18:163